Journal of Physics: Conference Series **2889** (2024) 012034 doi:10.1088/1742-6596/2889/1/012034

A compact cold atom cavity clock

A. Bregazzi[1], E. Batori[2], B. Lewis[1], C. Affolderbach[2], G. Mileti[2], P. Griffin[1] and E. Riis[1]

[1] Department of Physics, University of Strathclyde, G4 0NG, Glasgow, UK
[2] University of Neuchâtel, Institute of Physics, Laboratoire Temps-Fréquence, Avenue de Bellevaux 51, 2000 Neuchâtel, Switzerland

e.riis@strath.ac.uk

Abstract. A sample of laser cooled atoms are created inside an additively manufactured loop-gap microwave cavity using a grating magneto-optic trap requiring only a single laser cooling beam. Using a Ramsey excitation scheme with free evolution times of up to 20 ms and based on the ^{87}Rb ground-state clock transition, we demonstrate a short-term stability of $1.5\times10^{-11}\,\tau^{-1/2}$, averaging down to 2×10^{-12} after 100 s. The short-term stability limit is found to be dominated by the signal to noise ratio of the Ramsey fringes while for longer timescales the limitation is magnetic field noise due to the experiment being magnetically unshielded. Potential improvements to the setup and its operation point to a viable route forward for a miniaturised atomic microwave clock.

1. Introduction

Laser cooling and trapping of atoms and ions have brought substantial advantages to the field of atomic clocks. Most notably this is exemplified by the laser cooled atomic fountain [1,2], which currently provides the basis for the realisation of the SI second using a ground-state microwave transition in atomic Cs. Equally, a future redefinition is expected to take advantage of optical transitions in atoms cooled and trapped in optical fields, again taking advantage of a long interrogation of atoms in a pristine environment [3]. The drive towards improved clock stability, however, has led to ever increasing experimental complexity, size and laser performance requirements. This is contrasted by parallel development of optical-microwave double resonance clocks using hot vapour cells with applications expected in future portable, compact and space-grade clocks [4-7]. While impressive performance has been achieved, these systems are ultimately limited by coupling with fluctuating environmental parameters [4,8], vapour-cell ageing [9] and high dephasing rates. Vapour cell clocks based on coherent population trapping (CPT), where the chip-scale atomic clock [10] (CSAC) has achieved 10^{-10} level performance with low power consumption and an impressive small form factor, share these limitations.

In an effort to limit the impact of the operating environment and extend the possible interrogation time, solutions have been presented for compact cold atom microwave clocks based on spherical [11,12] and cylindrical cavities [13,14] as well as more recently on a loop-gap-resonator [15]. Common to these schemes and the one presented in this paper is that they all take advantage in the same way as the atomic fountain of the low perturbation environment cold atoms experience in free fall. However, they all have interrogation times in the 10s of ms region rather than the ~1 s flight time in a fountain [2]. While this does increase the observed atomic linewidth it vastly reduces the size of the apparatus and offers the potential for a reduced cycle time and hence increased data rate.

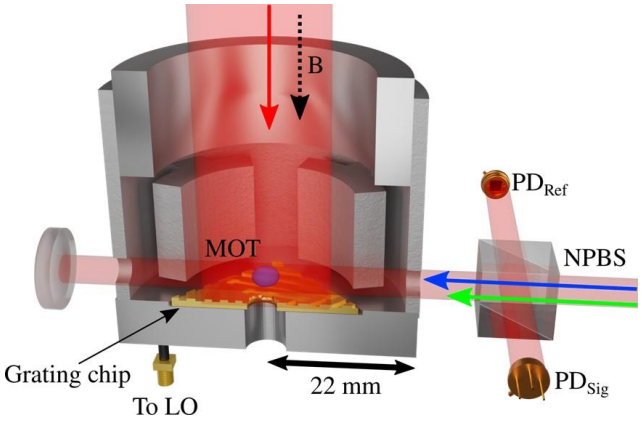

Figure 1. Simplified experimental setup showing cold atoms trapped inside loop-gap resonator. A single beam of laser cooling light (red arrow) impinges on the micro-fabricated grating at the bottom of the cavity forming the basis for the compact GMOT. State preparation and normalised atomic read-out (green/blue arrows) are obtained with a weak retroreflected beam from the side. The dashed black arrow indicates the direction of the bias magnetic field.

In this work we present a demonstration of an optically pumped cold-atom ^{87}Rb clock operating in the conventional dual-pulse Ramsey scheme and utilising an additively manufactured loop-gap resonator [16] and a grating magneto-optical trap [17] (GMOT). The relatively complex cavity structure would be difficult to realise with traditional machining techniques and is enabled using additive manufacturing, while the GMOT architecture reduces the complexity of the optical delivery system required to trap and cool an atomic cloud.

2. Experimental setup

The setup for the laser cooling and atomic clock part of the experiment is shown in Figure 1. The use of the GMOT simplifies the atomic trapping and cooling process as only a single beam of light is required while providing similar atom numbers and temperatures to conventional laser cooling schemes. In the present setup the GMOT provides the additional advantage that it lends itself to implementation inside the bore of a loop-gap resonator without the need to create further holes for cooling beams. The grating is placed at one end of the resonator with the bore size chosen at 20 mm to match the cooling beam diameter. This setup is typically demonstrated to trap > 3×10^6 atoms and cool them to below 10 μK [18]. The MOT coils are wound coaxially with and external to the resonator and the whole setup mounted inside a vacuum system maintained at a pressure of ~10^{-8} mbar and with resistively heated Rb metal dispensers providing a partial Rb pressure of ~10^{-9} mbar.

The internal electrode structure of the loop-gap resonator shown in Figure 1 allows for the realisation of sub-wavelength cavities and hence is the basis for a compact physics package. The control required in the manufacturing process to ensure repeatability and accuracy of the electrode structure is afforded by additive manufacturing. The material chosen for this resonator was $AlSi_{10}Mg$ and was demonstrated to lead to insignificant additional outgassing at the operational vacuum pressure [16].

The loop-gap resonator operates in a TE_{011}-like mode at a resonance frequency of 6.8347 GHz with the nearest cavity modes more than 1 GHz away. The design, simulation and testing of the loop-gap resonator including assessment of the field alignment and homogeneity are described in detail elsewhere [16]. Due to the presence of the grating at the bottom of the resonator the Q-factor is rather low at 360. However, this is seen as an advantage as it minimises the cavity-pulling effect.

The atomic states are prepared and read out optically and hence require additional laser beam access. This is done through two diagonally opposite 4 mm holes cut in the resonator with no significant observable effect on the microwave field. After trapping and cooling the atoms are optically pumped into the dark F = 2, m_F = 0 ground state while in free fall. This step relies crucially on the alignment of the linear polarisation of the light with the ~100 mG bias magnetic field along the resonator axis. This state preparation is then followed by two microwave π/2 pulses separated by a Ramsey time T_R of up to 20 ms, limited by the expansion and fall of the atomic cloud. The 200 μs long π/2 pulses have a power level of ~0.04 mW, demonstrating that the low cavity-Q is not a problem. Following this the F=2 and total populations are determined by observing the absorption of a probe beam aligned through the holes

in the cavity. Full details of this process including the relevant laser frequencies present at the different stages are provided elsewhere [19]. The experimental cycle is repeated at a rate of up to 7 Hz taking advantage of recapturing 80-90% of the atoms before they leave the GMOT optical overlap region [20].

The correct π/2 pulse parameters are obtained by observing the Rabi oscillations as the pulse area is increased through several times π [16]. This additionally acts a sensitive diagnostic on the microwave field homogeneity of the loop-gap resonator. As the cold atoms probe a volume of the resonator set by the size of the atom cloud, they experience the inhomogeneity of the microwave field amplitude and hence a variation of the Rabi frequency across the cloud. Experimentally this is observed as a dampening of the Rabi oscillation with a 1/e pulse area of ~10π. In terms of field inhomogeneity this corresponds to a 6.3% across the volume sampled by the atoms [16].

3. Results

Figure 2 shows an example of this normalised signal for a Ramsey time of 10 ms corresponding to a fringe linewidth of 50 Hz. The SNR is measure to ~110 at the steepest points on either side of the central fringe. This is expected to translate into an Allan deviation at 1 s of an oscillator stabilised to the atomic transition of 8.95×10^{-12} for a 10 ms Ramsey time [19].

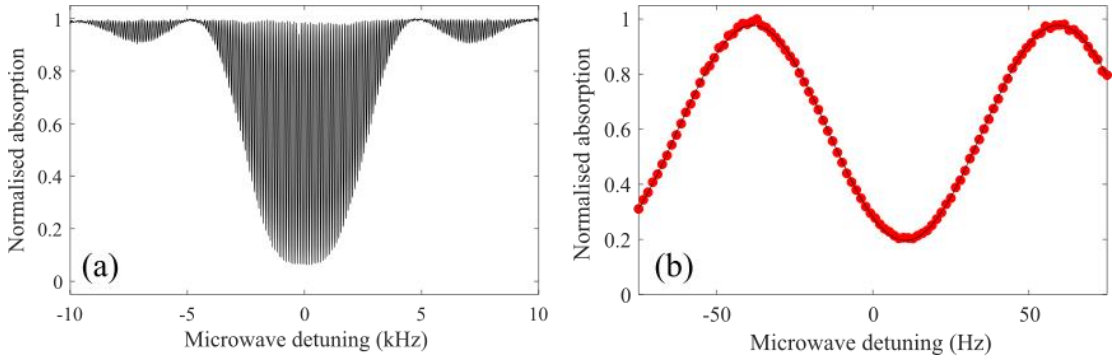

Figure 2. (a) Typical recorded Ramsey signal taken with a 10 ms free evolution time. (b) Closer look at the central Ramsey fringe obtained at 10 ms evolution time. Red points indicate measured normalised probe absorption while the black curve shows a sinusoidal fit to the data. The 100 mG bias field causes the observed fringe offset from 0 Hz detuning due to the second-order Zeeman effect.

To assess the stability of our system we lock the local oscillator frequency to the atomic signal. An error signal, which is used to steer the local oscillator through its internal reference, is obtained by jumping the microwave detuning between the steepest slopes on either side of the central fringe and comparing the recorded signal levels. The overlapping Allan deviation of the resulting atomic clock when compared to an oven-controlled quartz crystal oscillator disciplined to GPS is shown in Figure 3. The observed clock stability averages down with a $1.49\times10^{-11}\ \tau^{-1/2}$ dependence out to 10 s, where it starts deviating from the $\tau^{-1/2}$ dependence. The main reason for this is that the experiment is currently operating without magnetic shielding and as a result of that, magnetic field fluctuations will directly influence the clock stability through the second-order Zeeman effect. This has been confirmed by operating the clock on a first-order magnetic field sensitive transition ($|F = 1, m_F = 1\rangle \rightarrow |F' = 2, m_F' = 1\rangle$). The observed linear shift at 1.4 MHz/G on this transition can be converted for an equivalent field fluctuation to the expected effect on the second-order sensitive (575 Hz/G^2) clock transition. This is shown in the black curve in Figure 3 indicating that magnetic field fluctuations are a limiting factor for the stability in the 10s of seconds region.

At the 100s of seconds averaging time the clock stability is limited by the GPS disciplined quartz local oscillator. The Allan deviation of this oscillator is shown in the yellow curve in Figure 3. Together these two effects explain the observed levelling off of the Allan deviation of the cold atom microwave

clock at longer averaging times. However, in both cases there is a clear path to substantially reducing the effects through the inclusion of magnetic shielding and by the use of a lower-noise local oscillator.

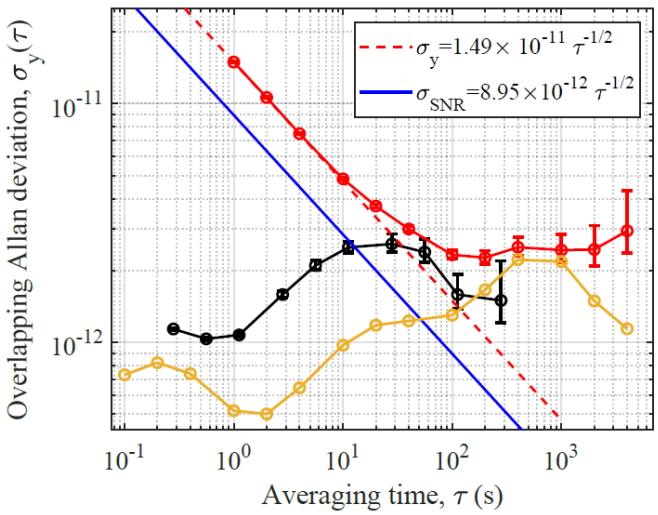

Figure 3. Red points: Overlapping Allan deviation of local oscillator when locked to the atomic signal. Red dashed line: $\tau^{-1/2}$ dependence of the measured 1 s stability. Blue solid line: stability expected from measured fringe SNR. Black points: stability limit set by observed magnetic field fluctuations through second-order Zeeman shift. Yellow points: GPS disciplined reference oscillator stability measured against two commercial Cs beam clocks (three-corner hat). Error bars represent 1σ confidence bound.

The stability budget at τ = 1 s is summarised in Table 1. The dominating identified source is the SNR of the observed absorption signal. At a value of ~110 this is about an order of magnitude worse than the quantum projection limit of the square root of the atom number. The primary route to approaching this limit is an optimisation of the detection process through the suppression of probe laser intensity and frequency noise.

The next most significant limitation to the 1 s clock stability is electronic noise on the signal used to steer the local oscillator. In the current setup this is not a major concern, but improvements to the SNR and shielded operation are expected to readily enable operation of the clock below the 10^{-12} level of this noise source and this would hence require further optimisation.

Table 1. The various identified noise sources and their contributions to the Allan deviation at 1 s integration time.

Noise source	σ contribution (τ = 1s)
SNR	8.95×10^{-12}
Electronic noise	1.14×10^{-12}
Dick Effect	6.12×10^{-13}
Zeeman Effect	1.07×10^{-12}
QPN	4.90×10^{-13}
Total $\left(\sqrt{\sigma_{SNR}^2 + \sigma_{Elec}^2 + \sigma_{Dick}^2}\right)$	9.04×10^{-12}
Measured	1.49×10^{-11}

Currently the Dick effect [21], which is a manifestation of local oscillator phase noise, is not a limiting factor but can be reduced further when solving the GPS disciplined reference oscillator stability problem evident in the data.

Overall, Table 1 demonstrates a reasonable agreement between the observed stability obtained at a 10 ms Ramsey time and the theoretical expectations of the identified main noise components based on separate analysis of their individual contributions.

4. Conclusion

We have implemented an additively manufactured loop-gap resonator in a compact microwave clock based on ^{87}Rb atoms cooled in a grating magneto-optic trap. In the present implementation the experimentally optimised clock stability is measured as $1.5\times10^{-11}\,\tau^{-1/2}$, averaging down to 2×10^{-12} after 100 s. The short-term stability is primarily limited by the SNR of the Ramsey signal. In the medium-term the clock stability is limited by the second-order Zeeman shift due to magnetic field noise while a further limit is due to the reference oscillator itself. Measures to reduce these limiting effects are outlined above. Additionally, it would be possible to extend the Ramsey time by an order of magnitude through implementing a low launch-height grating-chip fountain [22]. In a CPT clock experiment signals were observed from atoms returning after 100 ms. In addition to eliminating the issue of the atoms dropping out of view of the probe beam this would also have the advantage of the two Ramsey pulses probing the atoms in approximately the same location of the cavity. To gain the full advantage of this approach it may be necessary to lower the atomic temperature further, e.g. through the use of grey molasses, which has also been demonstrated at for a grating chip [23].

The loop-gap resonator inherently allows for a compact setup and the physics package is amenable to further miniaturisation and integration. The additive manufacturing process not only ensures a scalable manufacturing process, it has also recently been demonstrated to be compatibility with the requirements for vacuum chambers operating at UHV [24] pressure levels. This could potentially lead to the cavity body itself doubling up as a UHV chamber, enabling the entire physics package to be manufactured as a single component, thereby reducing the size and complexity of the system. Furthermore, passively pumped vacuum chambers have been shown to maintain the pressure required for atom trapping for extended periods of time [25,26]. The implementation of this would not only lead to a reduced power consumption by negating the continuous use of an ion pump but also a further reduction in size and the elimination of a permanent magnet. With a corresponding further integration of the lasers and optical manipulation requirements [27] there would appear to be a genuine opportunity to realise an integrated microwave clock benefitting from many of the cold-atom advantages of the atomic fountain, but trading off a small factor of stability for a vast reduction of experimental complexity and not least size, weight and power.

References

[1] Kasevich MA, Riis E, Chu S and DeVoe RG 1989 *Phys. Rev. Lett* **63** 612
[2] Bize S 2019 *Comptes Rendus Physique* **20** 153
[3] Dimarcq N *et al.* 2023 *Metrologia* in press https://doi.org/10.1088/1681-7575/ad17d2
[4] Almat N, Gharavipour M, Moreno W, Affolderbach C and Mileti G 2019 *Joint Conf. of the IEEE Intern'l Freq. Control Symposium & European Frequency and Time Forum* 1
[5] Batori E, Almat N, Affolderbach C and Mileti G 2020 *Adv. Space Res.* **68** 4723
[6] Huang M, Little A and Camparo J 2022 *Joint Conference of the European Frequency and Time Forum & IEEE International Frequency Control Symposium* 1
[7] Batori E, Affolderbach C, Pellaton M, Gruet F, Violetti M, Su Y, Skrivervik AK and Mileti G 2022 *Phys. Rev. Appl.* **18** 054039
[8] Moreno W, Pellaton M, Affolderbach C and Mileti G 2018 IEEE *Trans. Ultrason. Ferroelectr. Freq. Control* **65** 1500
[9] Abdullah S, Affolderbach C, Gruet F and Mileti G 2015 *Appl. Phys. Lett.* **106** 163505
[10] Knappe S, Shah V, Schwindt PDD, Hollberg L, Kitching J, Liew LA and Moreland J 2004 *Appl. Phys. Lett.* ***85*** 1460
[11] Esnault FX, Holleville D, Rossetto N, Guerandel S and Dimarcq N 2010 *Phys. Rev.* A **83** 033436
[12] Esnault F, Rossetto N, Holleville D, Delporte J and Dimarcq N 2011 *Adv. Space Res.* **47** 854
[13] Müller ST, Magalhães DV, Alves RF and Bagnato VS 2011 *J. Opt. Soc. Am.* B **28** 2592
[14] Liu P, Meng Y, Wan J, Wang X, Wang Y, Xiao L, Cheng H and Liu L 2015 *Phys. Rev.* A **92** 062101

[15] Lee S, Choi GW, Hong HG, Kwon TY, Lee SB, Heo MS and Park SE 2021 *Appl. Phys. Lett.* **119** 064002
[16] Batori E, Bregazzi A, Lewis B, Griffin PF, Riis E, Mileti G and Affolderbach C 2023 *Journal of Applied Physics* **133** 224401
[17] Nshii CC, Vangeleyn M, Cotter JP, Griffin PF, Hinds EA, Ironside CN, See P, Sinclair AG, Riis E and Arnold AS 2013 *Nature Nanotechnology* **8** 321
[18] McGilligan JP, Griffin PF, Elvin R, Ingleby SJ, Riis E and Arnold AS 2017 *Scientific Reports* **7** 384
[19] Bregazzi A, Batori E, Lewis B, Affolderbach C, Mileti G, Riis E and Griffin PF 2024 *Scientific Reports* **14** 931
[20] Hoth GW, Elvin R, Wright M, Lewis B, Arnold AS, Griffin PF and Riis E 2019 in *Proc. SPIE 10934, Optical, Opto-Atomic, and Entanglement-Enhanced Precision Metrology* eds. S. M. Shahriar and J. Scheuer (SPIE) 109342E
[21] Santarelli G, Audoin C, Makdissi A, Laurent P, Dick GJ and Clairon A 1998 *IEEE Transactions on Ultrason. Ferroelectr. Freq. Control* **45** 887
[22] Lewis B, Elvin R, Arnold AS, Riis E and Griffin PF 2022 *Appl. Phys. Lett.* **121** 164001
[23] Barker DS, Norrgard EB, Klimov NN, Fedchak JA, Scherschligt J and Eckel S 2022 *Opt. Express* **30** 9959
[24] Cooper N *et al.* 2021 *Addit. Manuf.* **40** 101898
[25] Little BJ, Hoth GW, Christensen J, Walker C, DeSmet DJ, Biedermann GW, Lee J and Schwindt PDD 2021 *AVS Quantum Sci.* **3** 035001
[26] Burrow OS, Osborn PF, Boughton E, Mirando F, Burt DP, Griffin PF, Arnold AS and Riis E 2021 *Appl. Phys. Lett.* **119** 124002
[27] Lee J *et al.* 2022 *Nature Comm.* **13** 5131

Acknowledgements
The authors would like to thank R. Elvin and J. P. McGilligan for useful conversations. A.B. was supported by a Ph.D. studentship from the Defence Science and Technology Laboratory (dstl). E. B., C.A. and G.M. acknowledge funding from the European space Agency (ESA, Contract No. 4000131046) and the Swiss Space Office (Swiss Confederation). We gratefully acknowledge funding from the UK Engineering and Physical Sciences Research Council through the International Network for Microfabrication of Atomic Quantum Sensors (EPSRC EP/W026929/1).